Current Biology, Vol. 12, 1256–1262, July 23, 2002, ©2002 Elsevier Science Ltd. All rights reserved. PII S0960-9822(02)00972-7

High-Resolution Structure of the Pleckstrin Homology Domain of Protein Kinase B/Akt Bound to Phosphatidylinositol (3,4,5)-Trisphosphate

Christine C. Thomas,[1] Maria Deak,[2] Dario R. Alessi,[2] and Daan M.F. van Aalten[1,3]
[1]Division of Biological Chemistry and Molecular Microbiology
[2]MRC Protein Phosphorylation Unit
School of Life Sciences
University of Dundee
Dundee DD1 5EH
Scotland
United Kingdom

Summary

The products of PI 3-kinase activation, PtdIns(3,4,5)P3 and its immediate breakdown product PtdIns(3,4)P2, trigger physiological processes, by interacting with proteins possessing pleckstrin homology (PH) domains [1, 2]. One of the best characterized PtdIns(3,4,5)P3/PtdIns(3,4)P2 effector proteins is protein kinase B (PKB), also known as Akt [3–5]. PKB possesses a PH domain located at its N terminus, and this domain binds specifically to PtdIns(3,4,5)P3 and PtdIns(3,4)P2 with similar affinity [6, 7]. Following activation of PI 3-kinase, PKB is recruited to the plasma membrane by virtue of its interaction with PtdIns(3,4,5)P3/PtdIns(3,4)P2 [8–10]. PKB is then activated by the 3-phosphoinositide-dependent protein kinase-1 (PDK1), which like PKB, possesses a PtdIns(3,4,5)P3/PtdIns(3,4)P2 binding PH domain [11, 12]. Here, we describe the high-resolution crystal structure of the isolated PH domain of PKB_α in complex with the head group of PtdIns(3,4,5)P3. The head group has a significantly different orientation and location compared to other Ins(1,3,4,5)P4 binding PH domains. Mutagenesis of the basic residues that form ionic interactions with the D3 and D4 phosphate groups reduces or abolishes the ability of PKB to interact with PtdIns(3,4,5)P3 and PtdIns(3,4)P2. The D5 phosphate faces the solvent and forms no significant interactions with any residue on the PH domain, and this explains why PKB interacts with similar affinity with both PtdIns(3,4,5)P3 and PtdIns(3,4)P2.

Results and Discussion

Overall Structure and Interaction with $Ins(1,3,4,5)P_4$

The structure of the pleckstrin homology domain of protein kinase B ($PKB_\alpha PH$) complexed to $Ins(1,3,4,5)P_4$ was solved by selenomethionine-MAD and yielded experimental phases to 1.4 Å resolution (Figure 1). Refinement of the structure resulted in a complete model for residues 1–113 (Figure 1). Well-defined density for $Ins(1,3,4,5)P_4$ allowed the construction of a model for this ligand in the binding pocket (Figure 1). The $PKB_\alpha PH$ structure reveals a standard PH domain fold [2], with seven β strands forming two orthogonal antiparallel β sheets, which are closed at one end by the C-terminal α helix. At the other end of the β barrel lie three loops (VL1–3) that are variable, both in sequence and length, in presently known PH domain structures [2]. These loops form a bowl lined with basic residues into which $Ins(1,3,4,5)P_4$ binds (Figures 1B and 2). The head group forms specific interactions with these basic residues and other side chains, and also with the protein backbone. The D1 phosphate forms relatively few interactions but interacts with Arg23 and the backbone nitrogen of Ile19 (Figure 1B). In contrast, the D3 phosphate interacts with four side chains, Lys14, Arg23, Arg25, and Asn53. This relatively large number of interactions with this phosphate group likely accounts for $PKB_\alpha PH$'s inability to bind with $PtdIns(4,5)P_2$, which lacks a D3 phosphate [6, 7]. Similarly, the D4 phosphate makes many interactions with Lys14, Asn53, and Arg86, and these interactions explain why $PKB_\alpha PH$ does not bind to PtdIns(3)P or $PtdIns(3,5)P_2$ [6, 7] (Figure 1B). Interestingly, the D5 phosphate does not interact with any protein atoms in the binding pocket. It is oriented toward the solvent and interacts only with five ordered water molecules. This explains the observation that PKB can interact with both $PtdIns(3,4)P_2$ or $PtdIns(3,4,5)P_3$ with similar affinity [6, 7].

Comparisons of $PKB_\alpha PH$ with the structures of the PH domains of BTK, DAPP1, and GRP1 in complex with $Ins(1,3,4,5)P_4$ (Figure 1B) show several key differences in the mode of interaction of $PKB_\alpha PH$ with $Ins(1,3,4,5)P_4$ that set it apart from these other PH domains. Firstly, the $Ins(1,3,4,5)P_4$ molecule in the $PKB_\alpha PH$ complex structure is in a different orientation than that observed in previous $Ins(1,3,4,5)P_4$-PH domain structures, and it is rotated approximately 45° in the plane of the inositol ring with respect to the orientation of the ligand in BTK, GRP1, and DAPP1 (Figure 1B). Secondly, the inositol ring appears to be shifted approximately 4 Å toward the core of the PH domain compared to the other $Ins(1,3,4,5)P_4$ complexes. As a result of these differences, there is a shift in the positioning of the phosphates and hence a difference in the number and type of interactions/contacts that are formed between the $Ins(1,3,4,5)P_4$ molecule and the pocket. The D5 phosphate and D6 hydroxyl group in the $PKB_\alpha PH$ complex are completely solvent exposed and are therefore incapable of forming the hydrogen bonds seen in the other structures between the D5 phosphate and the backbone of VL1. Overall, $PKB_\alpha PH$ appears to form fewer interactions with $Ins(1,3,4,5)P_4$ than the other PH domains, and this may account for the 10-fold lower affinity of $PKB_\alpha PH$ for $Ins(1,3,4,5)P_4$ compared to DAPP1, BTK, or GRP1 [11–13]. Another significant difference is that most of the residues that form key interactions between the PH domain and the D3 and D4 phosphates of $Ins(1,3,4,5)P_4$ are conserved; BTK, GRP1, and DAPP1 possess a conserved tyrosine residue (Tyr195 DAPP1, Tyr245 GRP1, Tyr39 BTK) within the binding site that interacts with

[3]Correspondence: dava@davapc1.bioch.dundee.ac.uk

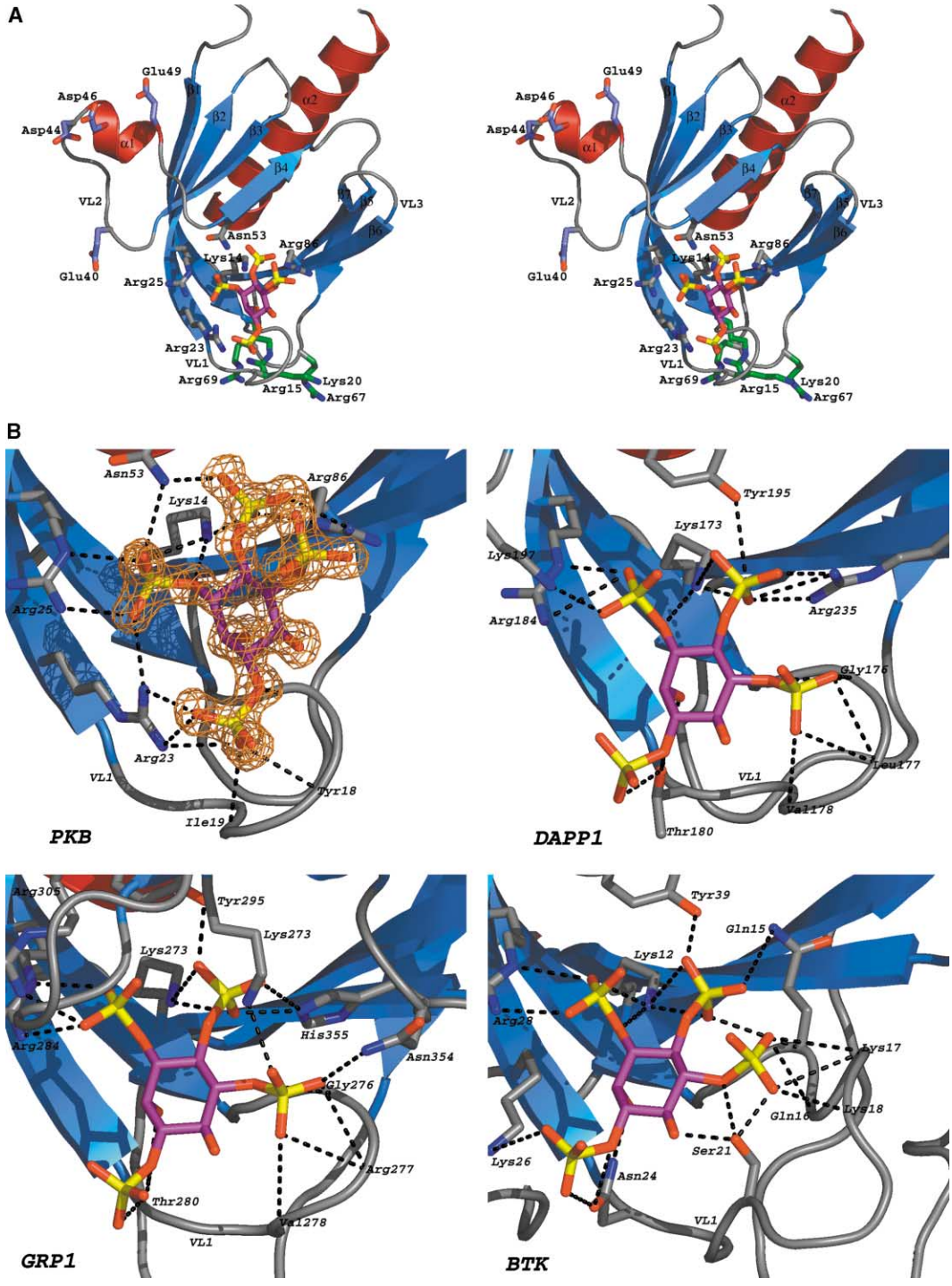

Figure 1. Structure of PKB$_\alpha$PH Complexed to Ins(1,3,4,5)P$_4$

(A) A ribbon drawing of the PKB$_\alpha$PH-Ins(1,3,4,5)P$_4$ complex, with the seven β strands (labeled β1–7) shown in blue and the α helices (labeled α1–2) shown in red. Ins(1,3,4,5)P$_4$ is shown as purple carbons. The side chains of residues interacting with this molecule are shown as gray carbons. The basic residues thought to interact with the membrane have their side chains shown as sticks with green carbons. The negatively charged residues on VL2 that are hypothesized to interact with the kinase domain are shown as gray-blue carbons.

(B) Ribbon diagrams of the Ins(1,3,4,5)P$_4$ binding sites of PKB, GRP1, DAPP1, and BTK. The Ins(1,3,4,5)P$_4$ is shown as purple carbons. For the PKB-Ins(1,3,4,5)P$_4$ structure, the experimental electron density map from SOLVE after density modification is shown in orange (contoured at 2.25σ). Residues that are hydrogen bonding the ligand are shown as sticks with gray carbons. Hydrogen bonds are shown as black dotted lines.

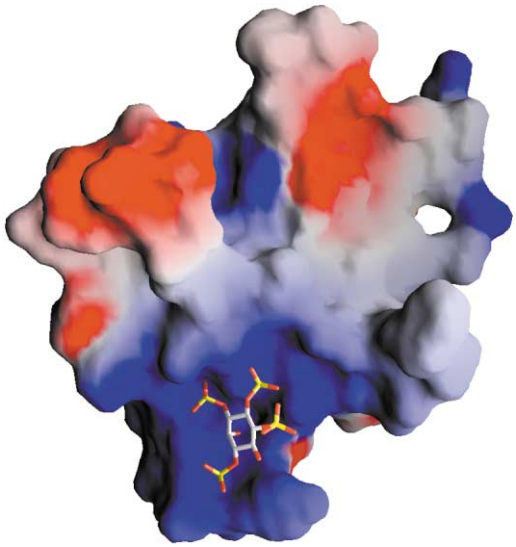

Figure 2. Charge Distribution

Electrostatic surface potential of PKB$_\alpha$PH-Ins(1,3,4,5)P$_4$ (calculated with GRASP), with the molecule in the same orientation as in Figure 1. Blue areas (+6kT) represent highly positively charged residues, and the red areas (−6kT) represent highly negatively charged residues. Ins(1,3,4,5)P$_4$ is shown as a stick model.

the D4 phosphate, which is not conserved in PKB$_\alpha$PH (Figure 3). The change in head group orientation and the absence of the tyrosine may provide key handles on the development of PKB$_\alpha$PH-specific inhibitors that do not interact with other PH domains.

Analysis of the electrostatic surface potential of the PKB$_\alpha$PH-Ins(1,3,4,5)P$_4$ complex shows that, apart from the phosphoinositide binding pocket, there is an additional area of clustered basic residues (Arg15, Lys20, Arg67, and Arg69) that do not participate in PtdIns binding. These residues form a flat, highly positively charged surface that could interact with the negatively charged lipid membrane (Figure 2). In a previous study, Tsichlis and colleagues observed that mutation of Arg15 to Ala significantly impaired the activation of PKB$_\alpha$ in PDGF-stimulated NIH3T3 cells [9]. This would be in agreement with Arg15 playing a key role in enabling PKB to interact with the membrane surface. In addition, in our model of how the PKB$_\alpha$ PH domain is oriented relative to the plasma membrane (Figures 1 and 2), the D1 phosphate is pointing down toward the membrane, and this orientation allows for binding of the inositol head group; however, the di-acyl glycerol backbone is still embedded in the hydrophobic core of the lipid bilayer, as would be expected for a PH domain-membrane interaction. This mode of interaction of the PH domain of PKB with PtdIns(3,4,5)P$_3$ at the plasma membrane results in two of the variable loops, VL2 and VL3, pointing away from the membrane, and this configuration provides possible docking sites for the PKB kinase domain that are free of steric hindrance from the membrane surface (Figures 1 and 2). VL3 (Figure 1A) forms a relatively short loop carrying uncharged side chains. In contrast, VL2 contains a high concentration of negatively charged residues (Glu40, Asp44, Asp46, and Glu49, Figures 1 and 2). This loop also contains a short α helix (Figure 1A), and the charged residues occupy one side of the helix and face away from the PH domain core, toward the solvent. A short α helix is observed in a similar location in the spectrin PH domain, both in the presence and absence of a head group [14, 15].

Mutagenesis of Residues in the Binding Pocket

The structure indicates that it is the interaction of PKB with the D3 and D4 phosphate groups of the inositol ring that is the key determinant for the binding of PtdIns(3,4,5)P$_3$ or PtdIns(3,4)P$_2$ to PKB$_\alpha$PH. To further investigate the molecular basis of the lipid binding specificity of the PH domain, we constructed several full-length PKB$_\alpha$ variants with mutations in the lipid binding pocket and evaluated their interaction with PtdIns(3,4)P$_2$ or PtdIns(3,4,5)P$_3$ using the protein-lipid overlay assay that has been used previously to assess the lipid binding properties of PKB and other PH domain-containing proteins [16–18] (Figure 4A). As reported previously, full-

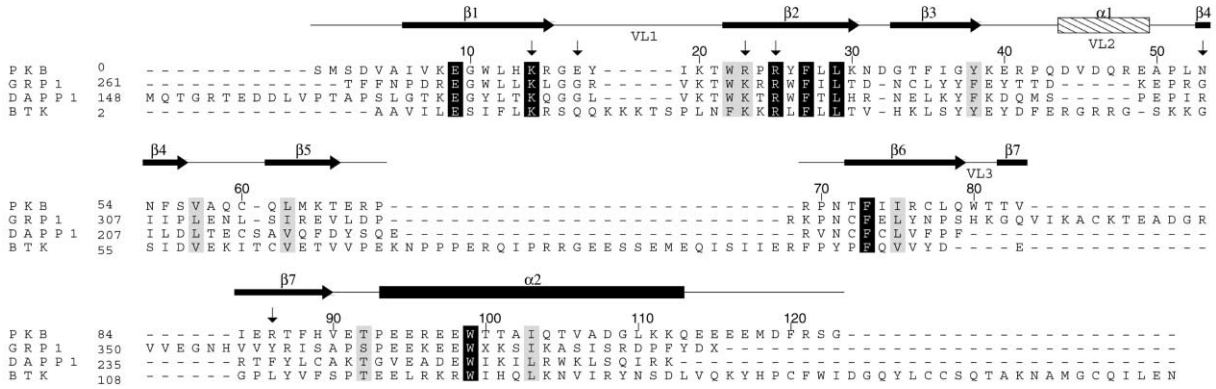

Figure 3. Structure-Based Sequence Alignment

The alignment of four PtdIns(3,4,5)P$_3$ binding PH domains, constructed by superposition of their structures with the MOTIF option in WHAT IF [31]. Conserved residues are shown in black. Homologous residues are highlighted in gray. The secondary structure is shown as black arrows for β strands and as bars for the α helices. Helix α1 is shown as a shaded bar. The arrows indicate residues in PKB$_\alpha$PH that interact with the lipid head group. Variable loops 1, 2, and 3 are labeled as VL1, VL2, and VL3, respectively.

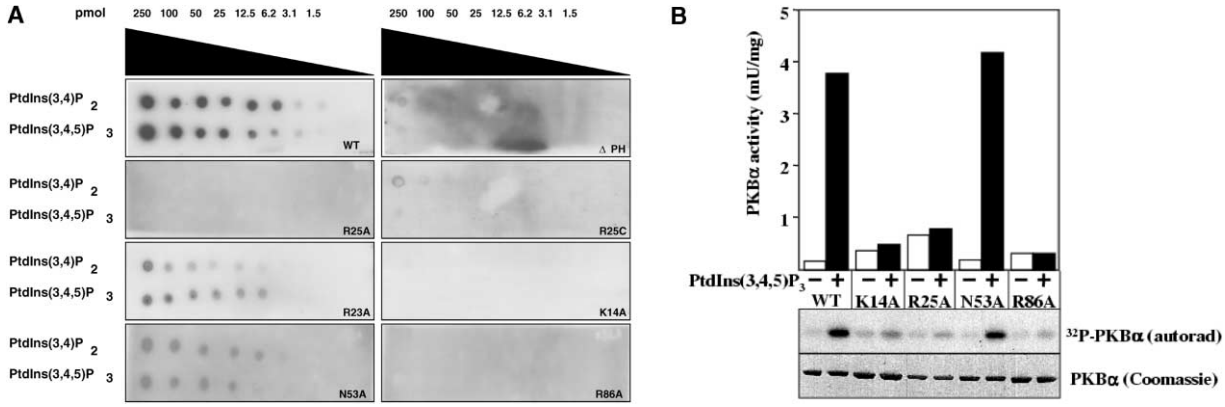

Figure 4. Mutant Analysis

(A) The ability of the wild-type and mutant GST-PKB$_\alpha$ fusion proteins to bind to the indicated amounts of PtdIns(3,4,5)P_3/PtdIns(3,4)P_2 was analyzed by using a protein lipid overlay assay [30].

(B) The ability of PDK1 to activate and phosphorylate the wild-type and mutant PKB$_\alpha$. The indicated forms of PKB$_\alpha$ were incubated with PDK1 magnesium and γ[^{32}P]ATP in the presence (+) or absence (−) of lipid vesicles containing PtdIns(3,4,5)P_3 as described previously [11]. The activation of PKB was assessed by its ability to phosphorylate the peptide substrate Crosstide (GRPRTSSFAEG). Phosphorylation of the AGC kinase substrate was determined following electrophoresis on a 4%–12% gradient polyacrylamide gel. The Coomassie blue-stained bands corresponding to each substrate were analyzed by autoradiography of the gel. Under the conditions used, phosphorylation of each substrate by PDK1 was linear with time and with the amount of enzyme added to the assay. Experiments were performed in duplicate, and similar results were obtained in two separate experiments.

length PKB interacted with both PtdIns(3,4,5)P_3 and PtdIns(3,4)P_2, but a mutant lacking the entire PH domain (ΔPH-PKB) did not detectably interact with these phosphoinositides (Figure 4). The affinity of PKB$_\alpha$ for the D1 phosphate was addressed by mutating Arg23 to Ala. The PKB$_\alpha$[R23A] was still capable of interacting with both PtdIns(3,4,5)P_3 and PtdIns(3,4)P_2, albeit with reduced affinity compared to the wild-type PKB$_\alpha$ mutant, and this indicates that the observed interaction of Arg23 with the D1 phosphate (Figures 1 and 3) plays a role in regulating the overall affinity of PKB for 3-phosphoinositides.

A more dramatic effect is observed when Arg25 (which binds the D3 phosphate, Figures 1 and 3) is mutated to

Table 1. Details of Data Collection and Structure Refinement for a MAD Data Set Collected on PKB$_\alpha$PH-Ins(1,3,4,5)P_4 Crystals

Structure	Peak	Inflection	Remote
Wave Length (Å)	0.97860	0.97896	0.96124
Space Group	C2	C2	C2
Unit Cell (Å)	a = 82.86	a = 82.86	a = 82.89
	b = 34.35	b = 34.36	b = 34.35
	c = 44.29	c = 44.30	c = 44.30
	β = 115.30°	β = 115.22°	β = 115.30°
Resolution (Å)	15–1.40 (1.45–1.4)	15–1.4 (1.45–1.4)	15–1.4 (1.45–1.4)
Observed Reflections	83,520	83,957	86,238
Unique Reflections	21,933	21,953	22,212
Redundancy	3.8 (2.6)	3.8 (2.6)	3.8 (2.8)
Completeness (%)	97.8 (83.3)	97.8 (83.0)	98.9 (90.5)
R_{merge}	0.055 (0.231)	0.052 (0.231)	0.058 (0.275)
I/σ I	30.8 (6.7)	30.8 (6.2)	29.77 (5.74)
R_{free} reflections	914		
R_{cryst}	0.125		
R_{free}	0.175		
Number of atoms			
Protein	958		
Water	160		
Ins(1,3,4,5)P_4	28		
Wilson B (Å^2)	16.9		
<B> Protein (Å^2)	13.3		
<B> Water (Å^2)	24.4		
<B> Ins(1,3,4,5)P_4 (Å^2)	9.1		
RMSD from Ideal Geometry			
Bond Lengths (Å)	0.010		
Bond Angles (°)	2.03		
Main Chain B (Å^2)	3.16		

The values between the parentheses are for the highest-resolution shell. All measured data were included in structure refinement.

either Ala or Cys (Figure 4). The binding of PtdIns(3,4)P_2 or PtdIns(3,4,5)P_3 to these mutants is almost completely lost, confirming the importance of this interaction in permitting PKB$_\alpha$ to bind Ptdins(3,4,5)P_3. Mutation of the equivalent Arg residue in the PH domain of the Bruton's tyrosine kinase has also been shown to prevent the interaction with PtdIns(3,4,5)P_3 [19]. The corresponding mutation in humans causes X-linked agammaglobulinaemia, an inherited immune disease [19, 20]. The complete loss of PtdIns(3,4,5)P_3 and PtdIns(3,4)P_2 binding to PKB$_\alpha$ is also observed when Lys14 (which interacts with both the D3 and D4 phosphate groups, Figure 1) or Arg86 (which interacts with the D4 phosphate group) are mutated to Ala (Figure 4). However, only a slight reduction in binding is observed for the Asn53Ala mutant (which interacts with the D3 and D4 phosphates). The qualitative data from the protein lipid overlay assays (Figure 4A) are confirmed by a more quantitative activation study (Figure 4B) in which the ability of PDK1 to phosphorylate and activate wild-type and mutant forms of PKB is measured in the absence and presence of PtdIns(3,4,5)P_3. The results from this study demonstrate that the mutants of PKB$_\alpha$ that are unable to interact with PtdIns(3,4,5)P_3 (PKB$_\alpha$[K14A], PKB$_\alpha$[R25A], and PKB$_\alpha$[R86A]) cannot be phosphorylated or activated by PDK1 in the presence of PtdIns(3,4,5)P_3. Together, the structure and the binding and activation studies on the mutants suggest that, in particular, the D3 and D4 phosphates play a key role in enabling PKB$_\alpha$ to interact specifically with PtdIns(3,4,5)P_3 and PtdIns(3,4)P_2, whereas the D1 phosphate plays only a supporting role. It is worth noting that, not only in native PKB$_\alpha$, but also in all mutants that we generated (Figure 4), PtdIns(3,4)P_2 and PtdIns(3,4,5)P_3 bind with similar affinity, further emphasizing that the D5 phosphate plays no role in mediating the binding of PKB$_\alpha$PH to phosphoinositides, in contrast to the PH domains of BTK, DAPP1, and GRP1, where this phosphate is known to be a key determinant of head group binding [13].

Conclusions

In this study, we have defined the key interactions that enable Ins(1,3,4,5)P_4 to bind PKB$_\alpha$PH. We explained why PKB can bind both PtdIns(3,4,5)P_3 and PtdIns(3,4)P_2 with equal affinity, due to absence of any ordered interactions with the D5 phosphate. A mutagenesis strategy, rationally designed on the basis of our structure, has shown that both the phosphates at D3 and D4 contribute the major share of the binding affinity. We have also shown that PKB$_\alpha$PH binds the lipid head group in a different mode from that observed in other PtdIns(3,4,5)P_3 binding PH domains.

Experimental Procedures

Cloning of PKB$_\alpha$PH

The phosphatidylinositide (PtdIns) binding pleckstrin homology (PH) domain of protein kinase B (PKB$_\alpha$PH) was amplified by PCR by using the Hi-fidelity PCR system with the full-length human PKB$_\alpha$ cDNA as the template and the 5′ primer 5′-GGATCCATGAGCGACG TGGCTATTGTGAAGGAG-3′ and the 3′ primer 5′-GGATCCTCAGC CCGACCGGAAGTCCATCTCCTC-3′. This amplified a length of DNA encoding residues 1–123 of human PKB$_\alpha$, with a stop codon immediately after codon 123 that is equivalent in length to the 3-phosphoinositide binding PH domains of DAPP1 [13] and TAPP1 [21] that have been crystallized previously. This fragment was subcloned into the BamH1 restriction site of the *Escherichia coli* expression vector pGEX4T-1. The resultant construct encodes for the bacterial expression of PKB$_\alpha$PH with an N-terminal glutathione-S-transferase (GST) tag.

Purification and Crystallization of Native and Selenomethionine PKB$_\alpha$PH

E. coli BL21 cells transformed with the pGEX4T-1 vector encoding the expression of GST-PKB$_\alpha$PH were grown at 37°C in 4 liters of Luria Bertani broth with 50 μg/ml ampicilin until OD_{600} reached 0.7. The expression of GST-PKB$_\alpha$PH was induced by the addition of 250 μM isopropyl-β-D-thiogalactopyranoside, and the bacteria were then grown for an additional 16 hr at 27°C. The cells were harvested by centrifugation at 3500 × g for 15 min, then lysed by resuspension in 200 ml buffer A (50 mM Tris/HCl [pH 7.5], 1 mM EGTA, 1 mM EDTA, 1 mM $NaVO_4$, 10 mM sodium-glycerophosphate, 50 mM NaF, 5 mM dithiothreitol) and "complete" proteinase inhibitor cocktail (one tablet per 25 ml; Roche) containing additional DNase (1.5–2 mg/ml) and 1 mg/ml lysozyme. The cells were then incubated on ice for 30 min before a final sonication step. The resulting solution was centrifuged at 14500 × g for 30 min to remove residual debris and was passed through a 0.45-μm filter. The supernatant was incubated for 1 hr at 4°C with 4 ml glutathione-Sepharose beads equilibrated against buffer A. The beads were then washed four times with five column volumes of buffer A and were subsequently washed six times with five column volumes of buffer B (50 mM Tris/HCl [pH 7.5], 0.1 mM EGTA, 0.3 M NaCl, and 5 mM dithiothreitol). The PKB$_\alpha$PH domain was then separated from the GST-tag by incubating the glutathione-Sepharose beads conjugated to GST-PKB$_\alpha$PH in a ratio of 2 units of thrombin to 10 μl resin at 4°C overnight. The resin was centrifuged and washed four times with 10 ml buffer B, and the combined supernatants containing PKB$_\alpha$PH were applied to a 0.2-ml benzamidine-agarose column to remove the thrombin. The eluate was subsequently applied to a 1-ml glutathione-Sepharose column equilibrated in buffer B to remove trace contamination of GST. The supernatant was then concentrated into a 4 ml volume and loaded onto a Superdex 75 26/60 gel filtration column that was previously equilibrated against buffer B. The yield obtained was approximately 5 mg PKB$_\alpha$PH domain per liter of *E. coli* culture. PKB$_\alpha$PH was analyzed by SDS-PAGE and was found to be essentially homogeneous. Further analysis by electrospray mass spectrometry revealed a major single species with a molecular mass of 14842.4, close to the predicted mass of 14752.6 for the PKB$_\alpha$PH fragment.

Selenomethionine-substituted protein was prepared by expressing protein in the methionine auxotrophic strain B834. Cells were grown overnight in Luria Bertani media and then further amplified in M9 minimal media supplemented with 1 g/l amino acid mix [22] lacking methionine. Adenine, guanosine, thymine, and uracil were added at 5 g/l, $FeSO_4$ was added at 4 mg/l, and $ZnCl_2$ was added at 40 mg/ml. The media was then filtered through a 0.22-μm filter, and L-selenomethionine was added to a final concentration of 125 mg/l. The cells were then grown to OD_{600} = 0.7 at 37°C, induced with IPTG as described above, and grown for an additional 16 hr at 27°C. Purification and crystallization proceeded as described for the native protein, and selenium incorporation was verified with electrospray mass spectrometry, revealing a major single species with a molecular mass of 14944, close to the predicted mass of 14872 for the selenomethionine-substituted PKB$_\alpha$PH fragment.

PKB$_\alpha$PH was concentrated to 8.5 mg/ml with a VivaSpin concentrator, and the concentration was verified at OD_{280}. The hanging drop vapor diffusion method was used for producing crystals. Hanging drops were formed by mixing 1 μl protein solution with 1 μl of a mother liquor solution. Selenomethione PKB$_\alpha$PH was complexed with Ins(1,3,4,5)P_4 by incubation in a 10:1 molar ratio of ligand to protein for 30 min on ice. The complex was crystallized using a mother liquor containing 0.25 M ammonium acetate, 30% PEG 4000, 0.1 M sodium acetate (pH 4.6). Monoclinic crystals (Table 1) appeared after 2 days and grew to approximately 0.2 × 0.2 × 0.3 mm after 4 days. Crystals were frozen in a nitrogen gas stream after being soaked in 10% 2-methyl-2,4-pentanediol for 30 s.

Data Collection, Structure Solution, and Refinement

A multiwavelength anomalous dispersion (MAD) data set for selenomethionine $PKB_{\alpha}PH$-Ins(1,3,4,5)P_4 was collected on Station 14.2 at the Daresbury Synchrotron Radiation Source with an ADSC Q4 CCD detector. The temperature of the crystals was maintained at 100K by using a nitrogen cryostream. Data were processed with the HKL package [23], and the statistics are shown in Table 1.

The structure of a $PKB_{\alpha}PH$ domain bound to Ins(1,3,4,5)P_4 was solved by MAD phasing with a three-wavelength experiment. Calculation of an anomalous Patterson with the peak wavelength data revealed a single 15σ peak. Two selenium sites were located and refined with SOLVE [24], and this refinement resulted in experimental phases to 1.4 Å with a figure of merit of 0.5, yielding a readily interpretable electron density map. Phases were further improved by density modification with DM [25], resulting in an electron density map that showed well-defined density for the protein and the Ins(1,3,4,5)P_4 molecule (Figure 1). The map was automatically interpreted with warpNtrace [26], which built 111 of a possible 123 residues and gave an initial protein model with $R = 0.323$ ($R_{free} = 0.324$). Iterative protein building in O [27] together with refinement in CNS [28] and incorporation of Ins(1,3,4,5)P_4 improved the model to $R = 0.277$ ($R_{free} = 0.289$). Refinement was then continued with SHELX-97, employing atomic anisotropic B factors and riding hydrogens as a last step, and this refinement resulted in the final model with $R = 0.125$ ($R_{free} = 0.175$), which encompassed residues 1–113.

Figures were made with PyMOL (http://www.pymol.org) and GRASP [29].

Characterization of PKB_{α} Mutants

The wild-type and mutants of PKB that were used for the lipid binding experiments were expressed in human embryonic kidney 293 cells and were purified as described before [11]. Lipid binding studies were carried out by using the protein-lipid overlay assay described previously [30]. Restriction enzyme digests, DNA ligations, Polymerase Chain Reaction cloning, and site-directed mutagenesis were performed by using standard protocols. All DNA constructs were verified by DNA sequencing (The Sequencing Service, School of Life Sciences, University of Dundee). All the phosphoinositides used in this study were dipalmitoyl derivatives obtained from Echelon. Hybond-C extra, the pGEX4T-1 vector, Enhanced Chemiluminescence reagent, thrombin protease, and glutathione-Sepharose were from Amersham Pharmacia Biotech; protease inhibitor tablets were from Roche; Benzamidine-Agarose and monoclonal anti-glutathione-S-transferase (GST) antibody were from Sigma; and the anti-goat anti-mouse horseradish peroxidase-conjugated secondary antibody was from Pierce.

Acknowledgments

We thank the European Synchrotron Radiation Facility, Grenoble, for the time at beamline ID29; the Daresbury Synchrotron Radiation Source for time and support on Station 14.2; Nick Morrice for performing mass spectra analysis; and the DNA Sequencing Service, School of Life Sciences, University of Dundee for DNA sequencing. C.C.T. is supported by a Biotechnology and Biological Sciences Research Council CASE studentship, D.M.F.v.A. is supported by a Wellcome Trust Career Development Research Fellowship, and D.R.A. is supported by the Medical Research Council (UK), Diabetes UK, Association for International Cancer Research, and the pharmaceutical companies supporting the Division of Signal Transduction Therapy unit in Dundee (AstraZeneca, Boehringer Ingelheim, NovoNordisk, Pfizer, GlaxoSmithKline Beecham).

Received: February 26, 2002
Revised: May 7, 2002
Accepted: June 12, 2002
Published: July 23, 2002

References

1. Isakoff, S.J., Cardozo, T., Andreev, J., Li, Z., Ferguson, K.M., Abagyan, R., Lemmon, M.A., Aronheim, A., and Skolnik, E.Y. (1998). Identification and analysis of PH domain-containing targets of phosphatidylinositol 3-kinase using a novel in vivo assay in yeast. EMBO J. *17*, 5374–5387.
2. Lemmon, M.A., and Ferguson, K.M. (2000). Signal-dependent membrane targeting by pleckstrin homology (PH) domains. Biochem. J. *350*, 1–18.
3. Brazil, D.P., and Hemmings, B.A. (2001). Ten years of protein kinase B signalling: a hard Akt to follow. Trends Biochem. Sci. *26*, 657–664.
4. Downward, J. (1998). Mechanisms and consequences of activation of protein kinase B/Akt. Curr. Opin. Cell Biol. *10*, 262–267.
5. Lawlor, M.A., and Alessi, D.R. (2001). PKB/Akt: a key mediator of cell proliferation, survival and insulin responses? J. Cell Sci. *114*, 2903–2910.
6. Frech, M., Andjelkovic, M., Ingley, E., Reddy, K.K., Falck, J.R., and Hemmings, B.A. (1997). High affinity binding of inositol phosphates and phosphoinositides to the Pleckstrin homology domain of RAC protein kinase B and their influence on kinase activity. J. Biol. Chem. *272*, 8474–8481.
7. James, S.R., Downes, C.P., Gigg, R., Grove, S.J.A., Holmes, A.B., and Alessi, D.R. (1996). Specific binding of the Akt-1 protein kinase to phosphatidylinositol 3,4,5-trisphosphate without subsequent activation. Biochem. J. *315*, 709–713.
8. Andjelkovic, M., Alessi, D.R., Meier, R., Fernandez, A., Lamb, N.J.C., Frech, M., Cron, P., Cohen, P., Lucocq, J.M., and Hemmings, B.A. (1997). Role of translocation in the activation and function of protein kinase B. J. Biol. Chem. *272*, 31515–31524.
9. Bellacosa, A., Chan, T.O., Ahmed, N.N., Datta, K., Malstrom, S., Stokoe, D., McCormick, F., Feng, J.N., and Tsichlis, P. (1998). Akt activation by growth factors is a multiple-step process: the role of the PH domain. Oncogene *17*, 313–325.
10. Watton, S.J., and Downward, J. (1999). Akt/PKB localisation and 3-phosphoinositide generation at sites of epithelial cell-matrix and cell-cell interaction. Curr. Biol. *9*, 433–436.
11. Alessi, D.R., Deak, M., Casamayor, A., Caudwell, F.B., Morrice, N., Norman, D.G., Gaffney, P., Reese, C.B., MacDougall, C.N., Harbison, D., et al. (1997). 3-phosphoinositide-dependent protein kinase-1 (PDK1): structural and functional homology with the *Drosophila* DSTPK61 kinase. Curr. Biol. *7*, 776–789.
12. Stephens, L., Anderson K., Stokoe, D., Erdjument-Bromage, H., Painter, G.F., Holmes, A.B., Gaffney, P.R., Reese, C.B., McCormick, F., Tempst, P., et al. (1998). Protein kinase B kinases that mediate phosphatidylinositol 3,4,5-triphosphate-dependent activation of protein kinase B. Science *279*, 710–714.
13. Ferguson, K.M., Kavran, J.M., Sankaran, V.G., Fournier, E., Isakoff, S.J., Skolnik, E.Y., and Lemmon, M.A. (2000). Structural basis for discrimination of 3-phosphoinositides by pleckstrin homology domains. Mol. Cell *6*, 373–384.
14. Hyvonen, M., Maclas, M.J., Nilges, M., Oschkinat, H., Saraste, M., and Wilmanns, M. (1995). Structure of the binding-site for inositol phosphates in a ph domain. EMBO J. *14*, 4676–4685.
15. Nilges, M., Macias, M.J., O'Donoghue, S.I., and Oschkinat, H. (1997). Automated NOESY interpretation with ambiguous distance restraints: the refined NMR solution structure of the pleckstrin homology domain from beta-spectrin. J. Mol. Biol. *269*, 408–422.
16. Kanai, F., Liu, H., Field, S.J., Akbary, H., Matsuo, T., Brown, G.E., Cantley, L.C., and Yaffe, M.B. (2001). The PX domains of p47phox and p40phox bind to lipid products of PI(3)K. Nat. Cell Biol. *3*, 675–678.
17. Krugmann, S., Anderson, K.E., Ridley, S.H., Risso, N., McGregor, A., Coadwell, J., Davidson, K., Eguinoa, A., Ellson, C.D., Lipp, P., et al. (2002). Identification of ARAP3, a novel PI3K effector regulating both Arf and Rho GTPases, by selective capture on phosphoinositide affinity matrices. Mol. Cell *9*, 95–108.
18. Dowler, S., Currie, R.A., Campbell, D.G., Deak, M., Kular, G., Downes, C.P., and Alessi, D.R. (2000). Identification of pleckstrin-homology-domain-containing proteins with novel phosphoinositide- binding specificities. Biochem. J. *351*, 19–31.
19. Hyvonen, M., and Saraste, M. (1997). Structure of the PH domain and Btk motif from Bruton's tyrosine kinase: molecular explanations for X-linked agammaglobulinaemia. EMBO J. *16*, 3396–3404.
20. Smith, C.I.E., Islam, K.B., Vorechovsky, I., Olerup, O., Wallin, E., Rabbani, H., Baskin, B., and Hammarstrom, L. (1994). X-linked

agammaglobulinemia and other immunoglobulin deficiencies. Immunol. Rev. *138*, 159–183.
21. Thomas, C.C., Dowler, S.J., Deak, M., Alessi, D.R., and van Aalten, D.M.F. (2001). Crystal structure of the phosphatidylinositol (3,4)-bisphosphate binding PH domain of TAPP1 - molecular basis of lipid specificity. Biochem. J. *358*, 287–294.
22. Alphey, M.S., Leonard, G.A., Gourley, D.G., Tetaud, E., Fairlamb, A.H., and Hunter, W.N. (1999). The high resolution crystal structure of recombinant *Crithidia fasciculata* tryparedoxin-I. J. Biol. Chem. *274*, 25613–25622.
23. Otwinowski, Z., and Minor, W. (1997). Processing of X-ray diffraction data collected in oscillation mode. Methods Enzymol. *276*, 307–326.
24. Terwilliger, T.C., and Berendzen, J. (1999). Automated MAD and MIR structure solution. Acta Crystallogr. D *55*, 849–861.
25. Cowtan, K. (1994). DM: an automated procedure for phase improvement by density modification. Joint CCP4 and ESF-EACBM Newslett. Protein Crystallogr. *31*, 34–38.
26. Perrakis, A., Morris, R., and Lamzin, V.S. (1999). Automated protein model building combined with iterative structure refinement. Nat. Struct. Biol. *6*, 458–463.
27. Jones, T.A., Zou, J.Y., Cowan, S.W., and Kjeldgaard, M. (1991). Improved methods for building protein models in electron density maps and the location of errors in these models. Acta Crystallogr. *A47*, 110–119.
28. Brunger, A.T., Adams, P.D., Clore, G.M., Gros, P., Grosse-Kunstleve, R.W., Jiang, J.-S., Kuszewski, J., Nilges, M., Pannu, N.S., Read, R.J., et al. (1998). Crystallography and NMR system: a new software system for macromolecular structure determination. Acta Crystallogr. *D54*, 905–921.
29. Nicholls, A., Sharp, K., and Honig, B. (1991). Protein folding and association - insights from the interfacial and thermodynamic properties of hydrocarbons. Proteins *11*, 281–296.
30. Dowler, S., Kular, G., and Alessi, D.R. (2002). Science STKE (www.stke.org).
31. Vriend, G. (1990). WHAT IF: a molecular modeling and drug design program. J. Mol. Graph. *8*, 52–56.

Accession Numbers

The coordinates and structure factors have been deposited with the Protein Data Bank (entry 1h10).